



ELSEVIER

Contents lists available at ScienceDirect

Chemical Engineering Science

journal homepage: www.elsevier.com/locate/ces

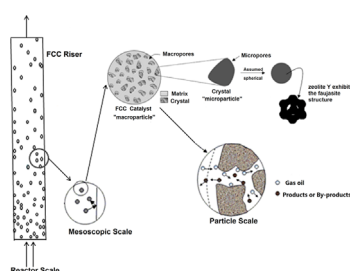
New insights into intraparticle transfer, particle kinetics, and gas–solid two-phase flow in polydisperse fluid catalytic cracking riser reactors under reaction conditions using multi-scale modeling

Guo-Qiang Chen^b, Zheng-Hong Luo^{a,b,*}^a Department of Chemical Engineering, College of Chemistry and Chemical Engineering, Shanghai Jiao Tong University, Shanghai 200240, PR China^b Department of Chemical and Biochemical Engineering, College of Chemistry and Chemical Engineering, Xiamen University, Xiamen 361005, PR China

HIGHLIGHTS

- New insights to the transport and reactor-scale effect on the FCC in riser reactors.
- Simultaneous transfer and FCC reaction, particle kinetics and flow are considered.
- A multi-scale model incorporates the CFD, single particle, FCC kinetics and PBM.
- The work demonstrated three catalytic and reactive operating zones in FCC risers.

GRAPHICAL ABSTRACT



ARTICLE INFO

Article history:

Received 25 November 2013

Received in revised form

7 January 2014

Accepted 11 January 2014

Available online 26 January 2014

Keywords:

Fluidization

Multiphase reactors

Granulation

Mathematical modeling

Multi-scale simulation

New insights into FCC riser reactor

ABSTRACT

This study provides new insights into fluid catalytic cracking (FCC) riser reactor from multi-scale viewpoint. The problem of simultaneous intraparticle molecule transfer and reaction, particle kinetics, and gas–solid flow in polydisperse FCC riser reactors was considered. A multi-scale CFD method was developed for constructing a multi-scale model to solve this problem. The multi-scale model consisted of a two-phase CFD model incorporating a single-particle model and a population balance model. The main flow field distribution parameters within the catalyst particles and reactors as well as the solid particle size distribution (PSD) could be calculated simultaneously based on intraparticle transfer and reaction using these models. The single-particle and multi-scale models were first verified and evaluated. Based on the validated models, intraparticle transfer limitations and/or flow fields in two size-scale FCC riser reactors were predicted. The simulations demonstrated three different reaction zones in FCC risers, and more elaborate mass, heat, and momentum transfer behaviors could be obtained. The simulations also demonstrated that particle kinetics (i.e., breakage and aggregation) have obvious influences on the FCC flow field in FCC risers; these effects have not been observed in conventional CFD models.

© 2014 Elsevier Ltd. All rights reserved.

1. Introduction

Fluid catalytic cracking (FCC) is an industrial process in which high molecular-weight hydrocarbons are converted into lower-

* Corresponding author at: Shanghai Jiaotong University, Department of Chemical Engineering, College of Chemistry and Chemical Engineering, Shanghai 200240, China. Tel./fax: +86 21 54745602.

E-mail address: luozh@sjtu.edu.cn (Z.-H. Luo).

molecular weight products of higher value. Approximately 45% of gasoline produced worldwide is obtained via the FCC process and its ancillary units (Xu et al., 2002). The key FCC reaction in the process is generally accomplished within short contact time-riser reactors, where the FCC catalyst is pneumatically conveyed by the hydrocarbon vapor from the bottom to the top of a vertical lifeline (Sadeghbeigi, 2000; Gao et al., 2008a, 2008b; 2009a, 2009b; Gan et al., 2011; Gilbert et al., 2011). Modern FCC riser reactors require to be handled a wide range of feedstocks and maximize light

olefins product for meeting market need (Chang et al., 2013). These changes significantly depend on a more comprehensive understanding of FCC riser reactors (Schwarz and Lee, 2007).

A typical FCC process (Fig. 1) proceeds by allowing contact between the vaporized feed and a solid zeolite catalyst after injection of the preheated liquid feedstock with steam through feed nozzles near the riser bottom. The feed vaporizes almost instantaneously to form vacuum gas oil (VGO) if it contacts with the hot catalysts. Thus, the FCC system can be handled as a gas–solid system (Wu et al., 2010; Pashikanti and Liu, 2011; Zhu et al.,

2011). The gas phase consists of VGO, by-products and products, whereas the solid phase consists of catalyst particles. Given that the fresh FCC catalyst particles enter the riser as a single component with particle size distribution (PSD), the solid phase can be characterized by PSD (Li et al., 2013), which can be directly linked to particle kinetics, i.e., particle abrasion, aggregation, and breakage, in the FCC process (Yan et al., 2012a, 2012b).

Catalytic cracking reactions occur in catalyst particles when they are exposed to the gas phase (Marroquin et al., 2005). The commercial FCC catalysts ($< 100 \mu\text{m}$) available are generally fabricated with $1\text{--}2 \mu\text{m}$ Y-zeolite crystals dispersed in a silica–alumina matrix, and only those hydrocarbon species with a kinetic diameter $< 10.2 \text{ \AA}$ can penetrate the zeolite pores (Venuto and Habib, 1979). FCC is a highly endothermic process involving complex intraparticle heat transfer phenomena that lead to an increase in intraparticle mass and heat transfer resistances. Knowledge of the solid PSD and intraparticle (diffusion and heat) transfer is necessary to understand the mixing effects inside a riser because these factors are expected to influence the reaction kinetics and the catalyst activity significantly (Karger and Ruthven, 1992; Chen et al., 2011; Lasa et al., 2011). Thus, different length scales (multi-scale) are involved in FCC risers because of the coupling of particle transfer and reaction (Bi and Li, 2004), and gas–solid FCC riser reactors are multi-scale structures (i.e., single catalyst particles, particle clusters/bubbles, and reactor) with multiple physical features (i.e., gas–solid flow hydrodynamics, particle kinetics, heat and mass transfer, and catalytic reaction kinetics; Fig. 2) (Bi and Li, 2004; Dompazis et al., 2008). Obtaining detailed models of such reactors is difficult because such models require a suitable reactor design, accounting for complex gas–solid flow, particle–particle and particle–reactor interactions, intraparticle transfer, and nanoscale phenomena, such as the kinetics of the catalyst active sites and intraparticle molecular transport and collision (Dompazis et al., 2008). A multi-scale CFD model based on the Euler–Euler method is necessary to address these complexities.

Most available works on FCC riser have concentrated on intraparticle transfer or gas–solid flow hydrodynamics in reactors,

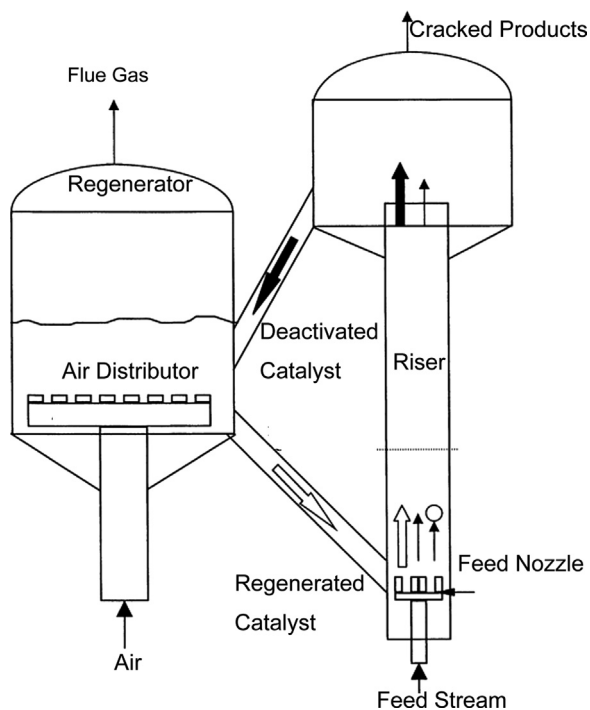


Fig. 1. Schematic diagram of FCC unit.

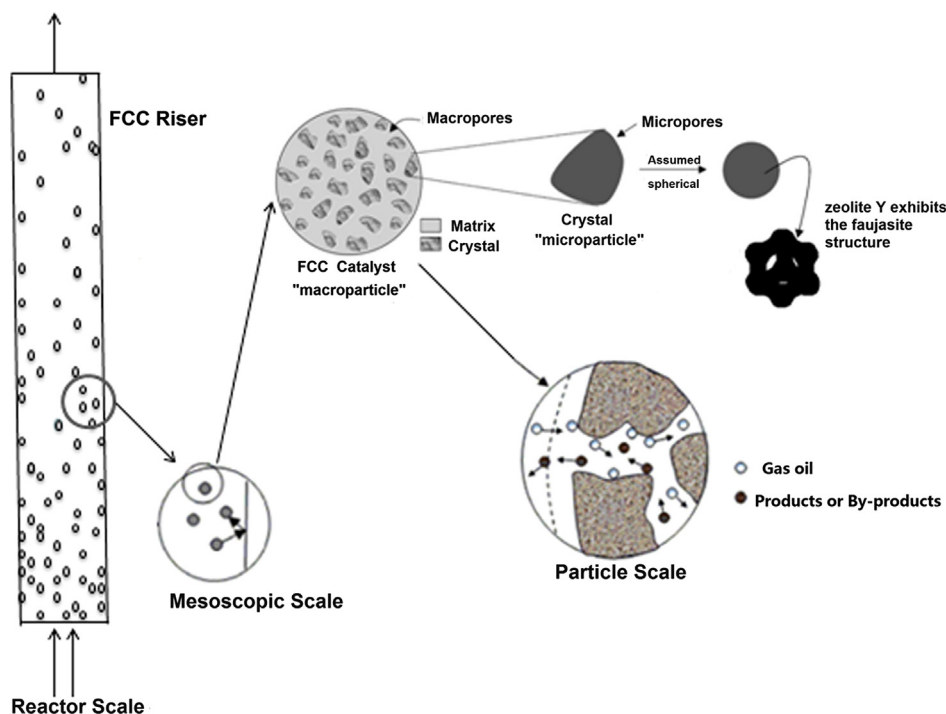


Fig. 2. The multi-scale phenomenon in the FCC riser reactor.

and few integrated studies have been conducted in this area. Nace (1970) experimentally investigated transfer limitations of gas molecules and their influences on FCC. Al-Khattaf and de Lasa (1999) calculated the effective diffusivity in Y-zeolites and demonstrated that diffusional constraints significantly affect primary FCC reactions. Wang et al. (2011) studied the limited intraparticle transfer of residual molecules at catalytic reaction condition. Chen et al. (2013) suggested a particle model to predict FCC intraparticle transfer behavior. The above works address these important phenomena of FCC intraparticle transfer but do not consider two-phase flow or catalyst PSD. Han and Chung (2001) developed a dynamic simulator to investigate the detailed dynamics of an FCC process. Nayak et al. (2005) computationally studied vaporization and cracking of liquid oil injected in a FCC riser reactor. Gao et al. (2008, 2009) investigated the hydrodynamics of binary mixture of particles in a turbulent FCC riser by experimentation and the CFD method. Vegendla et al. (2012) presented a hybrid solution algorithm to simulate an FCC riser using a 12 lumped-species reaction kinetic model. However, none of these studies addressed intraparticle transfer and PSD in FCC reactors. Dutta et al. (2012) recently simulated the hydrodynamic behavior of dispersed gas–solid flow in an industrial-scale FCC riser using the CFD approach incorporating the population balance model (PBM). Li et al. (2013) adopted a CFD–PBM coupled model to describe the turbulent gas–solid flow and reaction in a polydisperse FCC riser reactor. However, Dutta et al. and Li et al.'s works did not incorporate the intraparticle transfer model into their coupled model. Thus, intraparticle transfer limitations were still ignored in their studies (Dutta et al., 2012; Li et al., 2013).

The studies described thus far clearly demonstrate that early efforts on FCC riser reactors were directed toward the detailed aspects of intraparticle transfer (and reaction) and gas–solid flow with/without particle PSD. However, in practice, the two aspects are coupled (Kiss and Hudson, 2003). Comprehensive descriptions of behaviors encompassing simultaneous intraparticle transfer and reaction, gas–solid two-phase flow combined with solid PSD in the FCC reactor are also obviously neglected, as evidenced by the absence of multi-scale modeling of FCC risers in previous works.

Two approaches (i.e., sequential and iterative) have been used in multi-scale CFD modeling (Bi and Li, 2004). For sequential modeling, simulation data are simply passed from smaller scales to larger scales with no feedback (Bi and Li, 2004; Dollet, 2004). By contrast, an iterative model is coupled with different models at various scales to allow simultaneous interaction between scales (Bi and Li, 2004). Strong and complex interactions between elements/components at different scales in gas–solid catalytic reactors, including FCC risers, may be found; thus, information on transfer from larger scales to smaller scales is necessary. Considering its many features, the iterative multi-scale model is highly appropriate for describing such reactors. However, the multi-scale models currently available are mostly simple sequential models and few of these models are iterative ones (Kiss and Hudson, 2003; Li et al., 1999; Li and Kwauk, 2003; Bi and Li, 2004; Van den Akker, 2010). Wang and Li (2007) developed a classical mechanistic approach, i.e., the energy minimization multi-scale approach, to implement an iterative multi-scale CFD modeling in multi-phase reactors, wherein the variational criterion is formulated based on an evaluation of the compromise among interacting mechanisms.

The main objective of the present study is to obtain a more comprehensive understanding of FCC riser reactors from the chemical engineering viewpoint and provide new multi-scale insights into FCC riser reactors. A directly iterative multi-scale CFD simulation approach suggested by Luo et al. at Shanghai Jiao Tong University and Xiamen University (Chen et al., 2013) was adopted to construct a novel multi-scale CFD model for describing

simultaneous intraparticle transfer and reaction as well as gas–solid two-phase flow in polydisperse FCC riser reactors. The multi-scale model developed here utilizes a two-phase CFD model and combines a single-particle model and PBM. The main flow field distribution parameters within the catalyst particles and reactors are calculated while simultaneously accounting for intraparticle transfer and reaction and solid PSD using the multi-scale CFD model and its sub-models.

2. Model description

A novel multi-scale model based on an Eulerian–Eulerian two-fluid model incorporating a single-particle model and PBM was developed to describe the FCC reaction process realistically. Intraparticle transfer limitation, PSD, and gas–solid two-phase flow were considered simultaneously. Given that the three models are widely used in various two-phase reaction systems, they are described in brief in the Supporting information (see Supporting information for details). Herein, the selected FCC kinetic model (included in the single-particle model) is listed first because these multi-scale models and approaches are applied to the FCC reaction process in riser reactors. The concurrent multi-scale coupling procedure of the three models is then described.

2.1. Reaction kinetic model

With the fluid flow in the reactor, the FCC reaction occurs within catalyst particles. The FCC kinetic model should thus be incorporated into the single-particle model through the kinetic term, \mathfrak{R}_i , in Eq. (S5) and (S17). FCC reaction kinetics is remarkably influenced by the feedstock and catalyst employed. Mathematical models dealing with FCC kinetics can be categorized into two types. In the first category, the lumps are made on the basis of the boiling range of the feedstock and corresponding products in the reaction system. This type of models has an increasing trend in the number of lumps of gas components. In the second category, lumps are produced on the basis of the characteristics of the molecular structure of hydrocarbon groups in a reaction system. This category of models emphasizes detailed descriptions of feedstock (Wang et al., 2005). In both categories, the reaction kinetics considered is the “conversion” of one lump into another and not the “cracking” of an individual lump; the kinetic constants depend on the feedstock composition and must be determined for each combination of feedstock and catalyst.

Many lumped kinetic models have been successfully developed to describe the FCC reactions. For instance, the three-lump kinetic model was developed for VGO feed (Weekman and Nace, 1970), the four-lump kinetic model was developed by separating coke from the three-lump kinetic model (Lee et al., 1989), the six-lump kinetic model was developed for feed blended with vacuum residua (Takatsuka et al., 1987), and the ten-lump kinetic model was developed to consider other feed properties in addition to boiling range (Jacob et al., 1976). Other lumped kinetic models with greater complexity (Sha et al., 1985, 1995; Zhu et al., 1985) have also been described.

In the present work, the riser performance is simulated based on the four-lump kinetic model. The present simple kinetic model is suitable for predicting the effect of reactor feedback on the flow and reactor performance. Furthermore, the four-lump kinetic model is also easy to couple with material and energy balance equations as well as the single-particle model. The four-lump kinetic model based on the ultrastable submicron Y (USY) zeolite catalyst was developed by Gianetto et al. (1994). The values of the frequency factors and activation energies corresponding to the USY catalyst reported by Gianetto et al. were coupled with the

Table 1
Kinetic parameters for the 4-lump kinetic model.

Reactions	A_i^a	E_i^a /(J/mol)	ΔH_i^b /(J/mol)
K_1	$6.651(\pm 1.329)\times 10^4 \text{ m}^6/(\text{mol kg}_{\text{cat}} \text{ s})$	$9.820(\pm 0.128)\times 10^4$	195,000
K_2	$2.411(\pm 0.516)\times 10^6 \text{ m}^6/(\text{mol kg}_{\text{cat}} \text{ s})$	$1.261(\pm 0.014)\times 10^5$	670,000
K_3	$1.766(\pm 52.47)\times 10^5 \text{ m}^6/(\text{mol kg}_{\text{cat}} \text{ s})$	$1.324(\pm 2.228)\times 10^4$	745,000
K_4	$8.650(\pm 92.90)\times 10^2 \text{ m}^3/(\text{kg}_{\text{cat}} \text{ s})$	$1.137(\pm 4.284)\times 10^5$	512,500
K_5	$2.233(\pm 7.968)\times 10^1 \text{ m}^3/(\text{kg}_{\text{cat}} \text{ s})$	$5.912(\pm 2.546)\times 10^4$	550,000

$\phi(t_c) = e^{-\alpha C_0}$ $\alpha^c = 391 \pm 40 \text{ m}^3/\text{kmol}$

^cData from Berry et al. (2004).^a Data from Wu et al. (2009).^b Data from Nayak et al. (2005).**Table 2**
Model parameters and computational conditions.

Description	Value
Particle	
Diameter (m)	$7.0\text{e}-5^a$
Density (kg/m^3)	1500^a
Heat capacity ($\text{J}/\text{kg K}$)	1150^a
Thermal conductivity ($\text{W}/\text{m K}$)	0.0454^b
Curvature factor	3.617^c
Intraparticle porosity	0.3848^*
Average pore diameter (m)	$2.5409\text{e}-9^*$
Operating condition at inlet^d	
Gas temperature (K)	823
Catalyst temperature (K)	873
Gas flow rate ($\text{kg}/\text{m}^2\text{s}$)	6
Catalyst-to-oil ratio, CTO	10
Pressure (kPa)	25
Boundary conditions and model parameters	
Inlet boundary condition	Velocity inlet
Outlet boundary condition	Pressure outlet
Wall boundary condition	No slip for gas, part slip for solid
Wall thermal conditions	Adiabat
Near-wall treatment	Non-equilibrium wall functions
Particle-particle restitution coefficient	0.95
Particle-wall restitution coefficient	0.90
Granular viscosity	Gidaspow (1994)
Granular bulk viscosity	Lun et al. (1984)
Gravitational acceleration(m/s^2)	9.81
Transport and reaction	Volumetric Reaction (By UDF)
Solid phase packing limit	0.63
Time step(s)	10^{-3}
Convergence criteria	10^{-3}

^a Data from Wu et al. (2009).^b Data from Nayak et al. (2005).^c Data from Wang et al. (2011).^d Data from Wu et al. (2010).

* Data estimated from empirical equation (Chen et al., 2005).

two-dimensional reactor model for riser units by Berry et al. (2004) but poor predictions of the conversion and yields compared with the plant data were obtained. The model predictions were then improved by adjusting the activation energies for the reactions of gas oil consumption. More recently, Wu et al. (2009) performed two reasonable modifications on the four-lump kinetic model based on a re-evaluation of the kinetic parameters from available data. Finally, we obtained the kinetic parameters (Table 1) based on these three studies. The feed characteristics (Tables 3 and 4) and catalyst (Table 2) used in this work are similar to those employed in the three studies.

Table 3
Physical properties of each component.

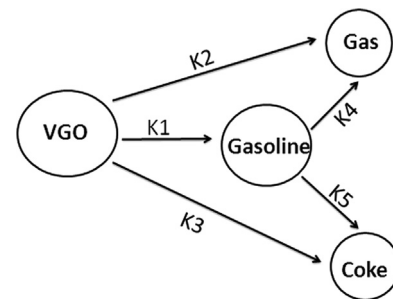
Component	Molecular weight (kg/kmol)	Specific heat ($\text{J}/\text{kg}/\text{K}$)	Viscosity ($\text{kg}/\text{m}/\text{s}$)
VGO	448	$C_p = A + B \frac{T}{1000}$ $+ C \left(\frac{T}{1000} \right)^2$	$5\text{e}-5$
Gasoline	112		$1.66\text{e}-5$
Gas	56		$1.66\text{e}-5$
Coke	448	510	$1.66\text{e}-5$

(1) Data from Wu et al. (2010), (2) Coke is treated as a component of gas phase with the same molecular weight with gas oil to eliminate its effect on the gas velocity. The same approach was used in Nayak et al. (2005).

Table 4
Mass heat capacity of fluid component.

Component	A_j	B_j	C_j
VGO	338.0	4920.7	-1717.6
Gasoline	296.2	5068.9	1788.8
Gas	382.6	5039.9	-1725.2

(1) Data from Wu et al. (2010) (2) The heat capacity of fluid component are calculated by the equations given in Table 3.

**Fig. 3.** The kinetic scheme used in this work.

The reaction scheme for the four-lump kinetic model can be found in Fig. 3. The four-lump kinetic model involves four simultaneous equations describing the evolution of unconverted gas oil lump (A), gasoline lump (B), light gas lump (C), and coke lump (D). The rate laws for gas oil reaction are second order with respect to the gas oil concentration, whereas the rate of gasoline decomposition is first order with respect to its concentration. The reaction rates for the four components are shown in Fig. 3; these rates are formulated as functions of the molar concentrations of the components in a certain step given as follows (Gianetto et al., 1994; Berry et al., 2004):

$$\mathfrak{R}_1 = -\phi(t_c)(K_1 + K_2 + K_3)C_1^2, \quad (1)$$

$$\mathfrak{R}_2 = \phi(t_c) \left(\frac{M_1}{M_2} K_1 - (K_4 + K_5) \right) C_2, \quad (2)$$

$$\mathfrak{R}_3 = \phi(t_c) \left(\frac{M_1}{M_3} K_2 + \frac{M_2}{M_3} K_4 \right) C_2, \quad (3)$$

$$\mathfrak{R}_4 = \phi(t_c) \left(\frac{M_1}{M_4} K_3 + \frac{M_2}{M_4} K_5 \right) C_2, \quad (4)$$

$$\phi(t_c) = e^{-\alpha C_4}. \quad (5)$$

The kinetic parameters are listed in Table 1 (Berry et al., 2004; Nayak et al., 2005; Wu et al., 2009).

2.2. Multi-scale modeling

To reproduce the FCC reaction process in a riser realistically, the single-particle model and PBM must be incorporated into the CFD model. The coupling scheme for the developed multi-scale model is shown in Fig. 4. The detailed description of Fig. 4 is as follows:

Step 1: QMOM is used to represent the FCC PSD. The weights (L_i) and abscissas ($p_{c,pi}$) show the mean diameter (L_{32}) and volume fraction of the solid phase (α_s). Step 2: The two-fluid model is initialized with the volume fraction calculated from Step 1. The governing equations are solved at every time step and grid point. From the two-fluid model, we can obtain the main parameters (e.g., pressure, temperature, species mass fraction, etc.). Step 3: Using the obtained parameters calculated from Step 2 as the boundary conditions, the single-particle model can be solved to obtain the real average volume reaction rates and reaction heat. Step 4: Interactively, the average volume reaction rates and reaction heat calculated from Step 3 are returned to solve the species transport equations and other related governing equations at the current solution of the CFD model. The flow field is then updated and Steps 2–4 are repeated for the next iteration.

The developed multi-scale model supposes that the grid inside a CFD model is sufficiently fine (grid independency analysis, Fig. 5 (c)) such that the parameter distribution within a single computational cell is minimal compared with that over the entire reactor and can be ignored and that the cell is the smallest unit that can be distinguished by the CFD model. Thus, all of the catalyst particles inside the same computational cell for the CFD model experience the same external conditions to ensure effective coupling of the

single-particle and CFD models. As a result, the single-particle model, the CFD model, and the PBM can be successfully coupled (the verification and evaluation of the coupled algorithm are found in Section 4.2). The developed multi-scale model, which considers both intraparticle transfer effect and particle size distribution, can accurately capture the gas–solid reaction flow behaviors usually missed by the pure conventional CFD model in FCC risers, thereby providing new insights. The application of this multi-scale model is described in detail below (Section 5).

3. Simulation conditions and modeling method

3.1. Simulated system and model parameters

To validate the efficiency and accuracy of the developed multi-scale approach/model, simulations of gas–solid reaction flows were performed in 2D domains for the laboratory-scale riser reactor described in Wu et al.'s work (2010). As described in Fig. 5(b), the width and height of the riser are 0.05 and 2.0 m, respectively. The model parameters and computational conditions are given in Table 2, the physical properties of each component are given in Tables 3 and 4, and the auxiliary equations for the gas mixture are given in Table 5. Tables 1 and 2 listed the simulation parameter values. The boundary conditions include (1) uniform velocity inlet boundary conditions, (2) pressure outlet boundary conditions, and (3) no slip/zero diffusive flux/zero heat flux wall boundary conditions.

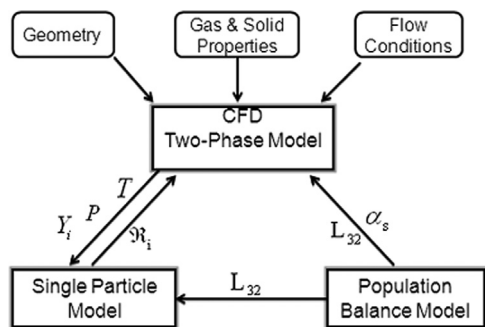


Fig. 4. The couple schematic of the multi-scale model.

Table 5
Auxiliary equations of gas mixture.

Item	Auxiliary equation
ρ	$\rho = \frac{P}{RT \sum Y_i / M_i}$
C_p	$2.52T + 981.0$
λ	$5.526e - 5T + 0.01155$
μ	$0.1672e - 5\sqrt{T} - 1.058e - 5$
M	$\frac{1}{\sum Y_i / M_i}$

The auxiliary equation from Gao et al. (1999).

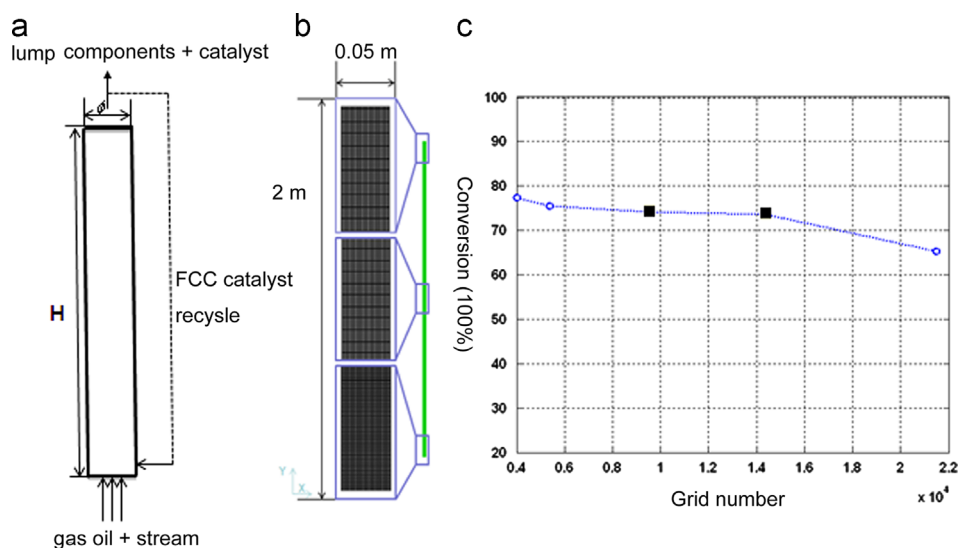


Fig. 5. FCC riser configurations diagram and grid independency ((a) Configuration diagram, (b) CFD grid, (c) Grid independency analysis).

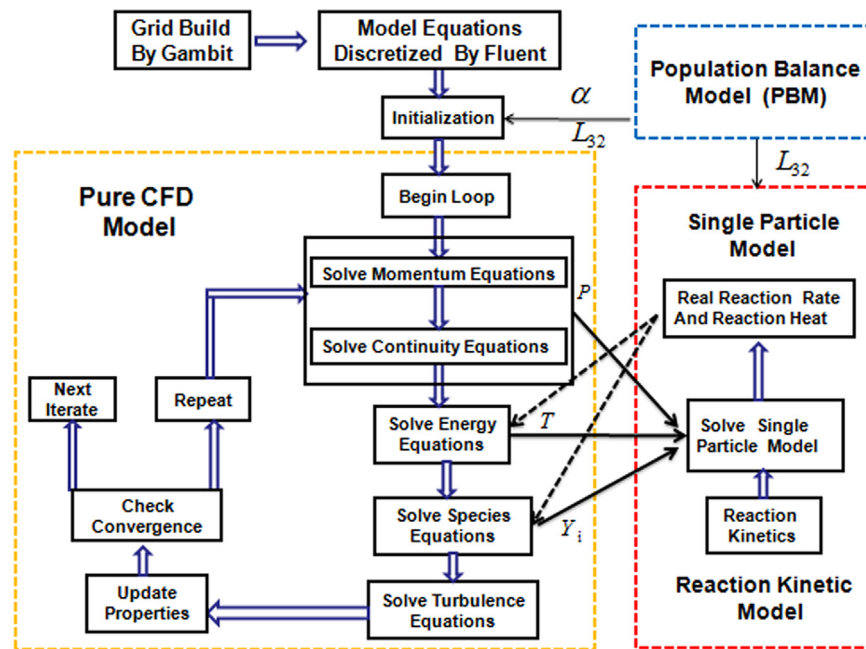


Fig. 6. Solution procedure of the multi-scale model.

3.2. Modeling method

The 2D simulations based on the multi-scale model were performed using the industrial CFD code FLUENT 6.3.26 (Ansys Inc., US) in double precision mode. In addition, a commercial grid-generation tool, GAMBIT 2.3.16 (Ansys Inc., USA) was used to generate the 2D geometries and grids. Initial grid independence studies indicate that a total of 9471 uniform cells (Fig. 5(c)) are sufficient to solve the multi-scale model accurately. The governing equations in the CFD model were discretized via uniform structural mesh using a finite-volume method. All of the field variables and their derivatives in a control volume were discretized using a second-order upwind method. Pressure and velocity were coupled with the SIMPLE algorithm and the sub-relaxation iteration method was used to ensure convergence. The governing equations in the single-particle model were solved using the orthogonal collocation method coupled with the Newton method. The equations and source terms of the single-particle model, the reaction kinetic model, Yang et al.'s drag model (2003), the perikinetic aggregation kernel, and other auxiliary equations of the gas mixture were incorporated into the CFD model using external user-defined functions (UDFs). Furthermore, the simulations were executed using a Dell T410 server platform with a 2.4 GHz Intel Xeon 4 CPU with 8 GB of RAM. Details of the entire computation process are shown in Fig. 6.

4. Model verification and evaluation

In this section, the predictive accuracy of the single-particle model is first verified, and the feasibility of the coupling method and reliability of the simulation results based on the multi-scale model are discussed.

4.1. Single-particle model verification

This section aims to verify the single-particle model. Herein, the effectiveness factor (defined by Eq. (6) (Solsvik and Jakobsen, 2011)), a dimensionless variable reflecting the extent of diffusion resistance within a catalyst, was calculated using the single-

particle model. The simulated data were compared with the estimated values obtained from the empirical formulas (Smith, 1981; Aris, 1969) listed in Eqs. (7) and (8).

$$\eta = \frac{\text{actual rate of action}}{\text{rate reaction with surface condition}} \quad (6)$$

$$\eta_i \approx \frac{\tanh(h'_i)}{h'_i} \quad (7)$$

where,

$$h'_i = \frac{1}{\alpha_{\text{ext}}} \sqrt{\frac{3k_{i,0}\rho_c\varphi_{\text{int}}c_{i,0}^{n-1}}{2}} \quad (8)$$

The FCC riser selected in this section is an industrial refinery, the Regina Refinery of Canada (1994). The single-particle model based on the catalyst position in the riser was solved using Matlab software. Simulation boundary conditions and actual parameter distribution data in the riser were collected from available reports (Ali et al., 1997; Han and Chung, 2001; Gupta and Rao, 2003; Berry et al., 2004; Wu et al., 2009; Sharma et al., 2011). Fig. 7(a) compares the simulation and estimated data obtained from the empirical equations, in which the simulated data were found to be consistent with the estimated data for the VGO reaction.

4.2. Evaluating the feasibility and accuracy of the coupling method

As discussed earlier, the predictive accuracy of single-particle model has been verified (Section 4.1). The pure conventional CFD model for the FCC riser reactor is widely implemented, and our group has performed FBR simulation research over several years and accumulated practical expertise in various aspects of this research field (Shi et al., 2010; Chen et al., 2011; Yan et al., 2011; Gao et al., 2011; Yan et al., 2012a, 2012b; Li et al., 2013). Herein, the feasibility of the coupling method and the accuracy of the multi-scale coupling model are analyzed as follows:

Step 1: The multi-scale model is solved using Fluent software, and the laboratory-scale riser reactor is simulated to obtain the steady-state flow field within the reactor. Simulation testing showed that 15 s, as a conservative estimate, is necessary to reach

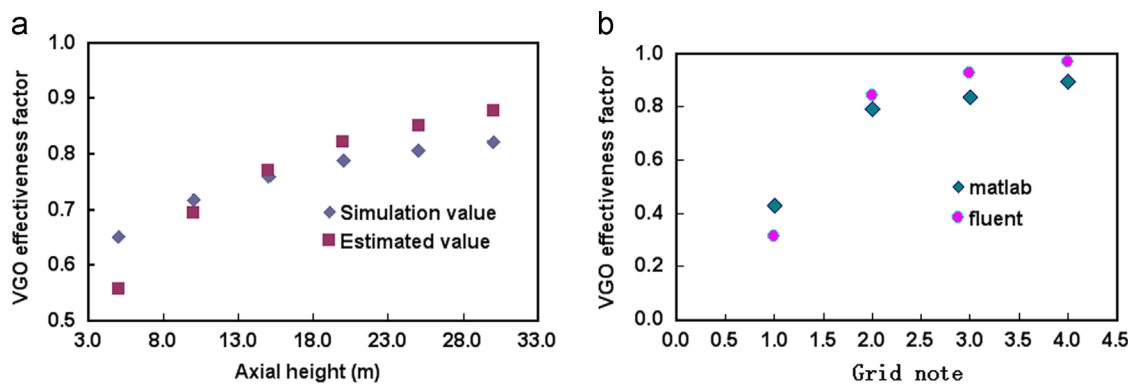


Fig. 7. Model validation and evaluation ((a) Single particle model, (b) Multi-scale model)).

Table 6

The boundary of grid nodes.

Cell	T/(K)	P/(kpa)	Y_{VGO}	$Y_{gasoline}$	Y_{gas}	Y_{coke}	Y_{H_2O}
1	768.6	2.476	0.717	0.153	0.078	0.002	0.05
2	768.5	2.470	0.485	0.306	0.072	0.087	0.05
3	749.5	2.468	0.372	0.385	0.182	0.011	0.05
4	745.2	2.467	0.270	0.452	0.210	0.018	0.05

steady-state conditions in the riser. Step 2: The multi-scale model is initialized with the parameter distributions obtained at $t=15$ s as described in Step 1. Typical grid points are chosen as shown in Table 6, the next iteration is performed in Fluent, and the effectiveness factor is obtained in this iteration. Step 3: Using the same parameter distributions at $t=15$ s as in the boundary condition, the single-particle model is solved using Matlab software, and the obtained effectiveness factors are compared with those obtained via Fluent software, described in Step 2.

Fig. 7(b) compares simulation values obtained from Matlab and Fluent software. The simulation values obtained using the two methods are basically identical. Therefore, the effectiveness factors calculated using the pure single-particle model are consistent with those obtained using the multi-scale model, which demonstrates that the coupling between the single-particle model and the CFD model is successful and that the calculation accuracy of the multi-scale is reliable.

5. Results and discussion

In this section, the single-particle model was first applied to an industrial-scale FCC riser. An investigation of the intraparticle transfer effect based on different catalyst positions in the riser was performed. The multi-scale model was then applied to a laboratory-scale riser. Three cases were considered: (i) the pure CFD model coupled directly with the reaction kinetic model (Case 1); (ii) the case (i) model coupled with the single-particle model (Case 2); and (iii) the case (ii) model coupled with the PBM (Case 3). Reactive flows with and without intraparticle transfer effects were compared, and the effect of intraparticle transfer with the PSD on VGO reaction rate, product yield, feed conversion, etc., were analyzed.

5.1. Intraparticle transport phenomena

Fig. 8 illustrates the main parameter differences between the surface and the center of a single FCC catalyst particle along the axial direction of the industrial-scale riser caused by intraparticle transfer limitations. As described in Fig. 8(a) and (b), significant

temperature and pressure differences may be found between the particle surface and its center, which indicates the existence of intraparticle transfer resistances. The intraparticle transfer effect decreased along the axial direction of the riser and was significant in the bottom section ($H < 10$ m), relatively weak in the middle section ($10 \text{ m} < H < 20$ m), and weakest in the upper section ($20 \text{ m} < H < 33$ m) of the riser. These three different zones could also be distinguished based on VGO concentration (Fig. 8(c)). Therefore, three different zones may be identified in risers based on intraparticle transfer effects along the axial direction; these zones are the transport-controlled, reaction-controlled, and intermediate transition zones (Fig. 8(d)).

The effectiveness factors for VGO reactions at different heights along the axial direction were also calculated to confirm the validity of the zone divisions. The effectiveness factor is a dimensionless quantity that describes intraparticle transfer effects on the FCC reactions (for a more detailed definition, see Section 4.1); larger deviations of this value from 1.0 indicate stronger effects caused by intraparticle transfer limitation. For the VGO reaction, a meso-scale definition of the different reaction zones in the riser could be established on the basis of the different values of the effectiveness factor given in Fig. 8(d). For instance, the transport-controlled zone ($0 < \eta_0 < 0.69$), the reaction-controlled zone ($0.80 < \eta_0 < 0.90$), and the intermediate transition zone ($0.69 < \eta_0 < 0.80$) could be defined (Chen et al., 2013).

In summary, the single-particle model offers new insights into the fundamental meso-scale mechanism of catalytic cracking, and details of the mass and heat transfer phenomena within the catalyst particle could be obtained. The basic sub-model underlying the multi-scale model may also be identified. This sub-model shows significant effects on the flow field distributions compared with conventional CFD models without considering intraparticle transfer effects and captures realistic reaction behaviors in FCC risers.

5.2. Multi-scale transport and reaction phenomena

5.2.1. Two-phase flow behavior

L_{32} is an important output variable directly related to particle size; thus, it affects flow fields in reactors via the PBM. The relationship between particle size and flow fields is reflected clearly by the volume fraction distribution of catalyst particles. Fig. 9 illustrates the transient PSD in the riser for Case 3 at different times. Fig. 9 shows that the multi-scale model captured particle breakage and aggregation phenomena that are usually missed by conventional CFD models. At the initial stage, the PSD was relatively narrow ($t < 0.5$ s). Two large changes in PSD were then found at 0.5–1.0 s and 1.0–3.0 s. In practice, the PSD increases because of particle breakage and aggregation. After 3.0 s, the change in particle size was relatively small. A wider PSD could

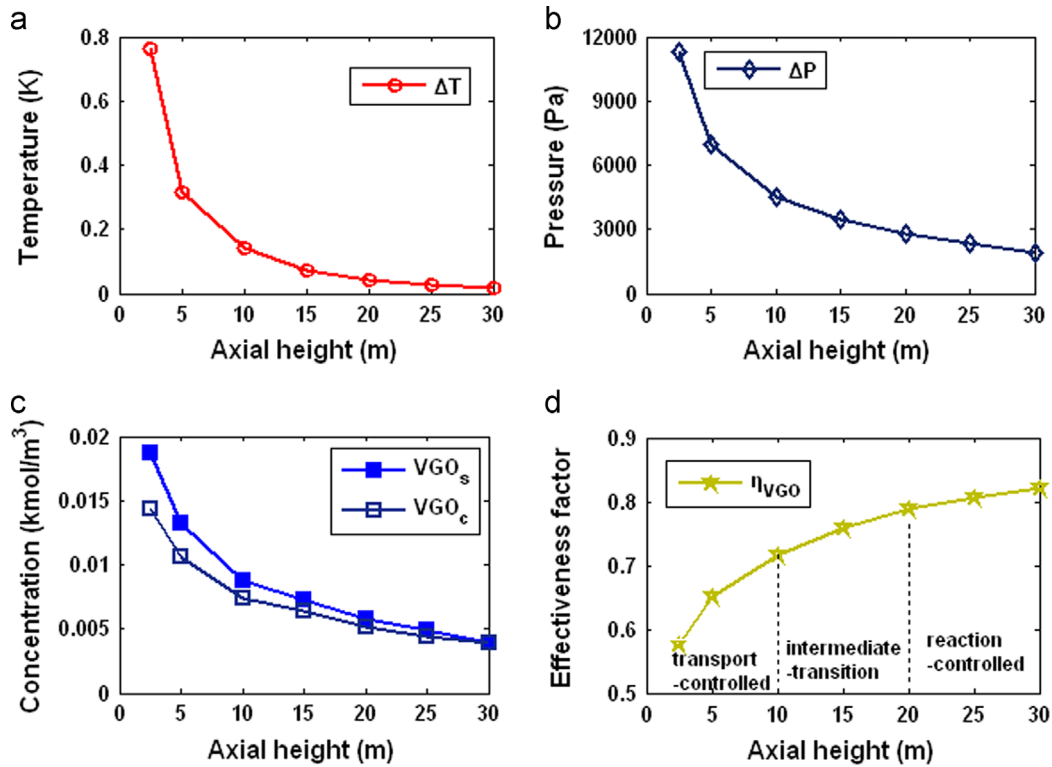


Fig. 8. The intraparticle transfer effect along the riser height ((a) Temperature differences between the surface and the center of the particle, (b) Pressure differences between the surface and center of the particle, (c) VGO concentration difference (VGO_s : the VGO concentration on the surface of the particle, VGO_c : the VGO concentration on the center of the particle), (d) VGO effectiveness factor).

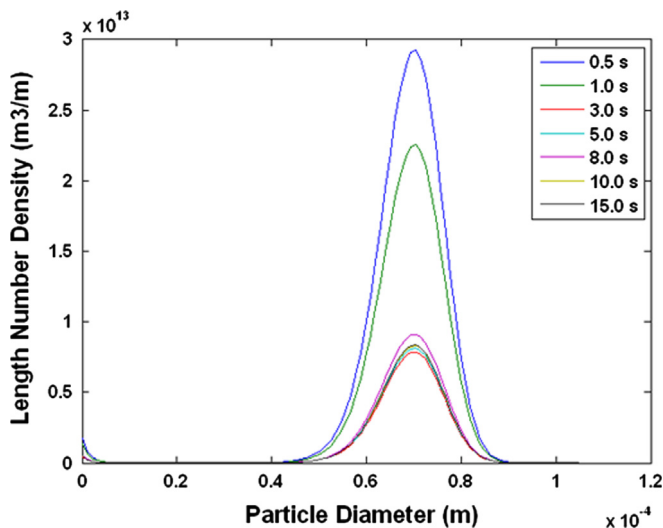


Fig. 9. PSDs in the FCC riser reactor in case 3 at different time spots.

be observed from Fig. 9 at these time points compared with those in the initial stage.

To demonstrate the particle breakage and aggregation phenomena more clearly, the spatial distributions of particle volume fraction in Cases 2 and 3 were also calculated (Fig. 10). Particle breakage and aggregation are shown in Fig. 10. The particle volume fraction distributions in the riser in Cases 2 and 3 were almost identical for $t < 0.5$ s. With increasing gas–solid fluidization, significant differences were found because of particle breakage and aggregation, and these differences corresponded well with the PSD (Fig. 9). Fig. 10 also shows that the particle breakage and aggregation effect was more obvious in the middle-upper section than in the bottom section of the riser. The particle volume

fraction was similar in the bottom section, whereas obvious particle aggregation (3.0 s to 8.0 s) and breakage (5.0 s to 10.0 s) were observed in the middle-upper section (Fig. 10). The particle volume fraction in Case 3 was larger than that in Case 2 in the middle-upper section. The multi-scale model captured particle breakage and aggregation phenomena in the industrial FCC process that cannot be predicted by conventional CFD models. Therefore, the multi-scale model more realistically and elaborately predicts flow field information in FCC risers than single-particle models. Detailed differences in time-averaged (15–30 s) flow field distributions obtained by the multi-scale model are presented in Figs. 11–13.

Fig. 11 shows the particle volume fraction profiles. The particle volume fraction decreased to a stable state along the axial direction in the riser (Fig. 11(a)). At the same axial position in the riser, the particle volume fractions near the wall region (annulus) were larger than those at the center (core), which indicates that the radial particle volume fraction distribution profile exhibits a “core-annulus” shape (Fig. 11(b)–(d)), thereby agreeing with previous theoretical and experimental results (Sadeghbeigi, 2000; Xu et al., 2002). The qualitative trends predicted in Cases 1 to 3 were similar, which further demonstrates that the multi-scale model has good qualitative prediction capability for simulating an actual riser. Fig. 11 shows that the entire volume fraction in Case 1 (pure CFD model) was larger than that in Case 2 (CFD model with intra-diffusion effect) both in the axial and radial directions in the riser. For the axial profiles, the particle volume fraction in Case 3 (CFD model with intra-diffusion and PSD effects) was larger than that in Case 2 (with intra-diffusion effect only) in the middle-upper bottom sections of the riser; these fractions were similar in the bottom section for both cases. For the radial profiles, the distributions were almost identical at the center region in the bottom section of the riser, whereas significant differences were found near the wall region and in the

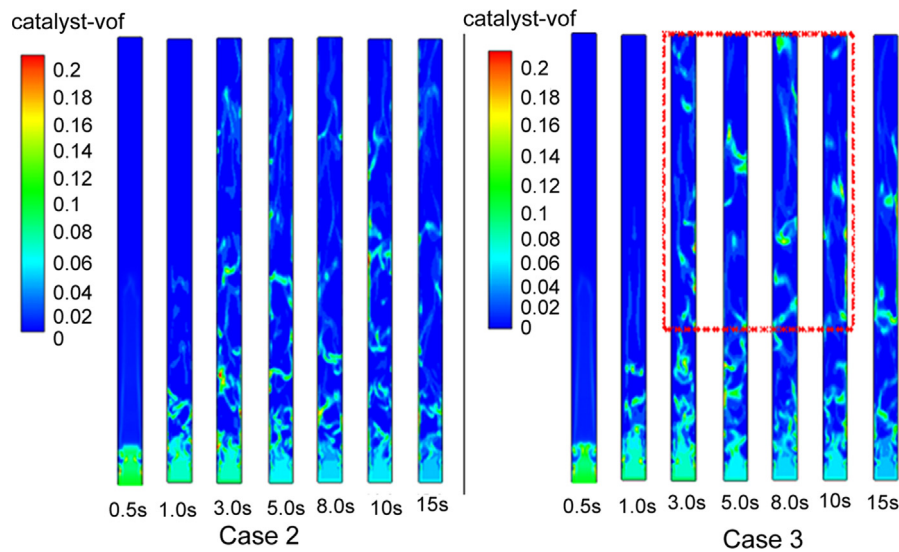


Fig. 10. The particle volume fraction in the FCC riser reactor at different time spots.

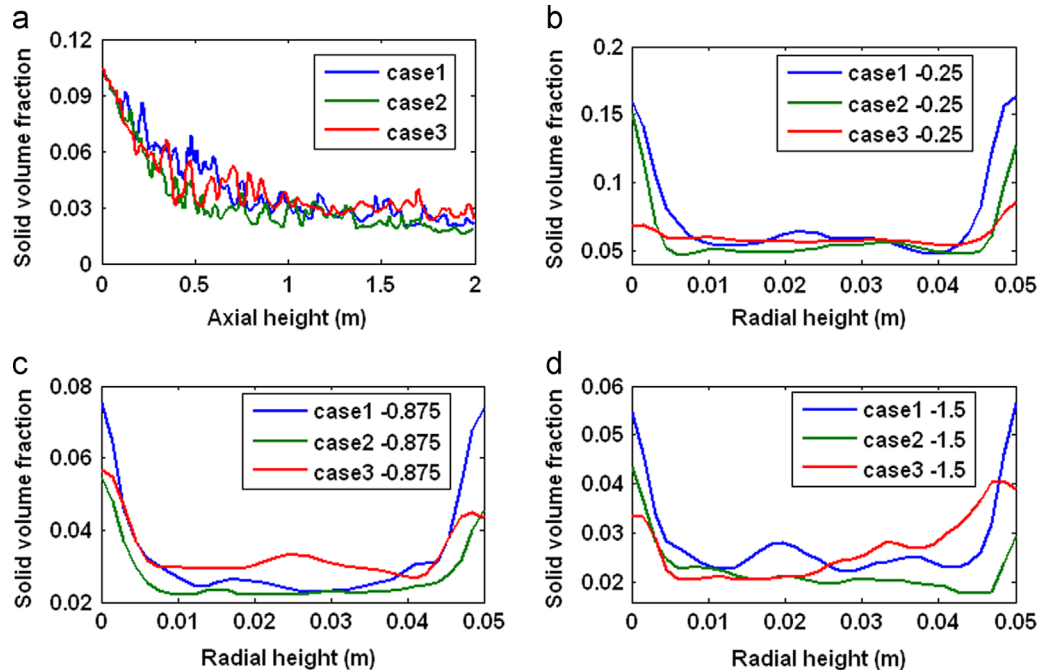


Fig. 11. The particle volume fraction profiles ((a) Axial distribution, (b–d) radial distribution).

middle-upper section (Fig. 11(b)–(d)). The distribution in Case 1 was larger than that in Case 3 at the bottom of the riser but smaller in the middle-upper sections. In particular, the particle volume fraction in Case 2 along the radial direction was larger than that in Case 3 near the wall region and similar to Case 3 at the center region of the riser in the bottom section. By contrast, the particle volume fraction in Case 3 was larger than that in Case 2 in the middle-upper section. The particle volume fraction in Case 1 was larger than that in Case 3 near the wall region and relatively smaller at the center region of the riser. These results could be explained by the flow behaviors described in Fig. 10 and further prove that intraparticle transfer limitations have significant effects on the two-phase flow behavior. The PSD also showed more significant effects on the flow field in the middle-upper section of the riser than in any other section. Therefore, the qualitative results predicted via the multi-scale model differ from those

predicted via the pure CFD model. The intraparticle transfer effect, PSD, and gas–solid two-phase flow should be considered simultaneously to capture the actual fluid dynamics in FCC risers.

Fig. 12 describes the calculated time-averaged phase velocity profiles. After the apparent acceleration period in the riser bottom section, both gas- and solid-phase velocities in the riser changed into a fully developed profile, which then became constant (Fig. 12(a), (b)). The phase velocity exhibited a parabolic distribution profile that was high at the riser center and relatively low near the wall region (Fig. 12(c), (d)). Solid downflow at the wall region could also be observed in Fig. 12(d). The two-phase velocity profiles matched well with the literature data (Sadeghbeigi, 2000; Xu et al., 2002), which further proves that the multi-scale model could accurately predict the flow field behavior in the riser. Fig. 12 also shows that the gas-phase velocity in Case 1 was larger than that in Case 2, whereas the solid-phase velocities in both cases

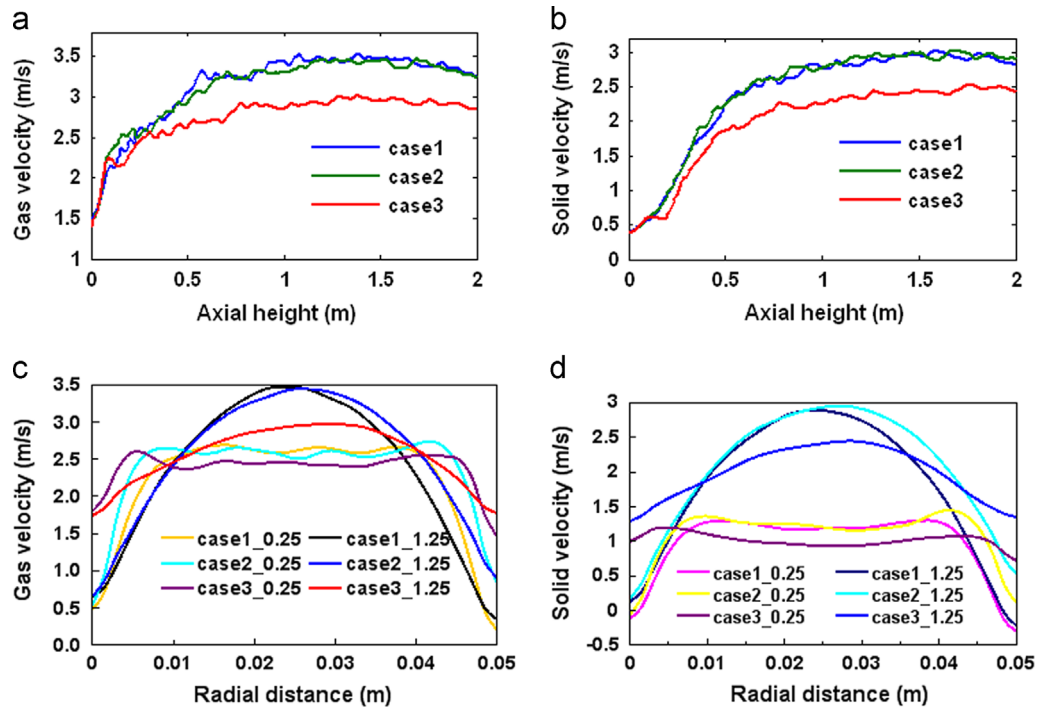


Fig. 12. The gas and solid phase velocity profiles ((a–b) Axial profiles, (c–d) radial profiles).

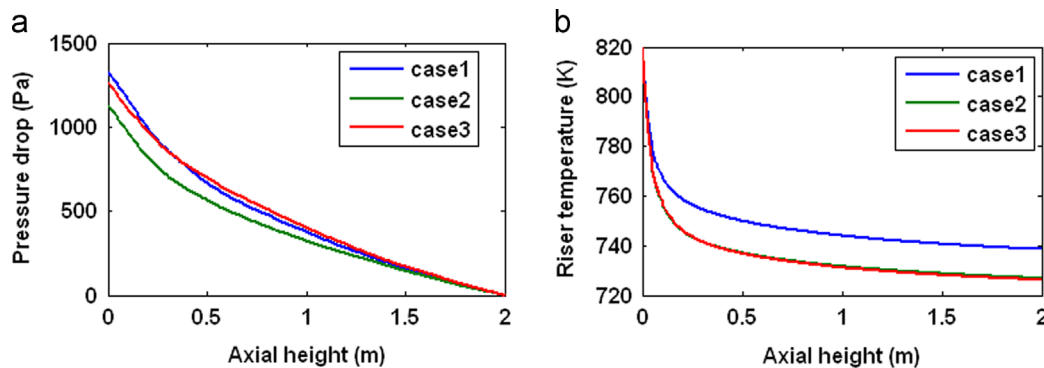


Fig. 13. The profiles along the riser height ((a) pressure drop profiles and (b) temperature profile).

were similar (Fig. 12(a), (b)). Given that the cracking reaction rates in Case 1 (without intra-diffusion resistance) were faster than those in Case 2 (with intra-diffusion resistance), the gas velocity in Case 1 was larger. The velocity of the solid phase is controlled simultaneously by many factors, such as the interaction forces between phases, its own weight, friction, and collision. The solid volume fraction in Case 1 was larger than that in Case 2. All of these factors contributed to the solid-phase velocity profiles described in Fig. 12(b). Fig. 12(a) and (b) also show that the two-phase velocity in Case 3 was obviously lower than that in Case 2, which could also be explained by the results obtained in Fig. 11(a). Here, the particle volume fraction in Case 3 was larger than that in Case 2, which leads to larger resistance against acceleration. In summary, the gas and solid velocity distribution profiles (Fig. 12) demonstrate that the qualitative results predicted using the multi-scale model are reliable and different from those predicted using the CFD model.

Fig. 13 shows the predicted time-averaged pressure drop and temperature profiles, which are qualitatively consistent with the results reported in literature (Sharma et al., 2011). Obvious differences captured by the multi-scale model could also be

observed. Fig. 13(a) shows that the pressure drops in Cases 1 and 3 were larger than that in Case 2, which is due to the variation in particle volume fraction (Fig. 11(a)). Fig. 13(b) shows that the temperature in Case 2 was lower than that in Case 1, whereas that in Case 2 was slightly higher than that in Case 3. As described in Section 5.1, obvious temperature gradients exist within the particle because of intraparticle transfer limitation. Accordingly, both the reaction temperatures in Cases 2 and 3 were smaller than that in Case 1 without intraparticle transfer limitations. The particle aggregations in Cases 2 and 3 were relatively more significant than in Case 1, thereby increasing intraparticle transfer resistance within the particle clusters. In addition, the particle concentration was relatively larger. These phenomena resulted in deeper reactions and lower temperatures.

The simulation results demonstrate that the multi-scale model has good qualitative predictive capability for simulating an actual FCC riser. Given that the multi-scale model incorporates a single-particle model to consider the intraparticle transfer limitation and the PBM to consider the PSD, more elaborate flow behaviors in the industrial FCC process, such as the intraparticle molecule transfer and reaction and the particle breakage or aggregation, could be

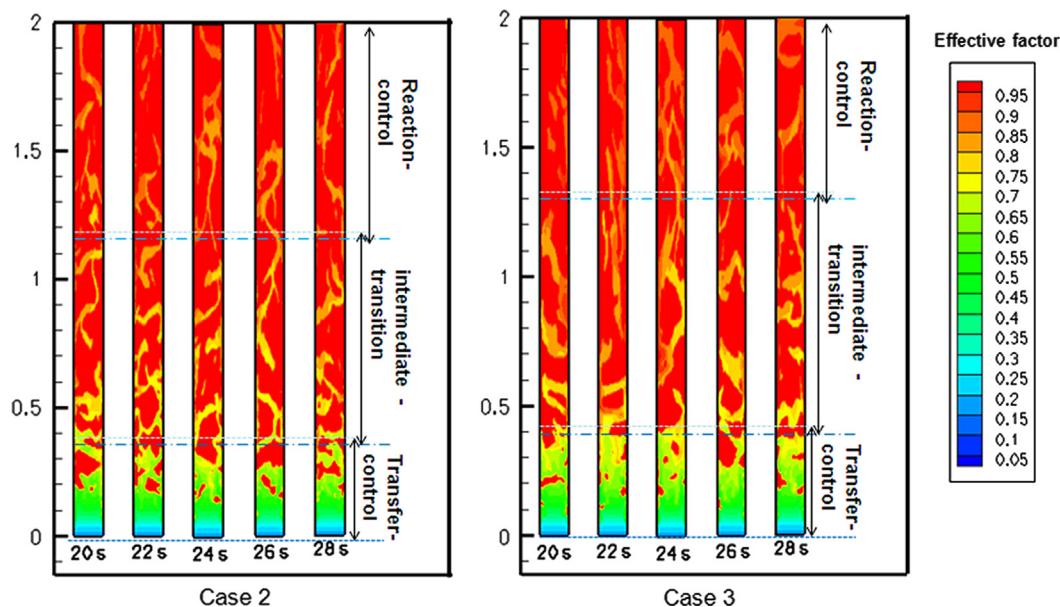


Fig. 14. The VGO effectiveness factor profiles along the riser height.

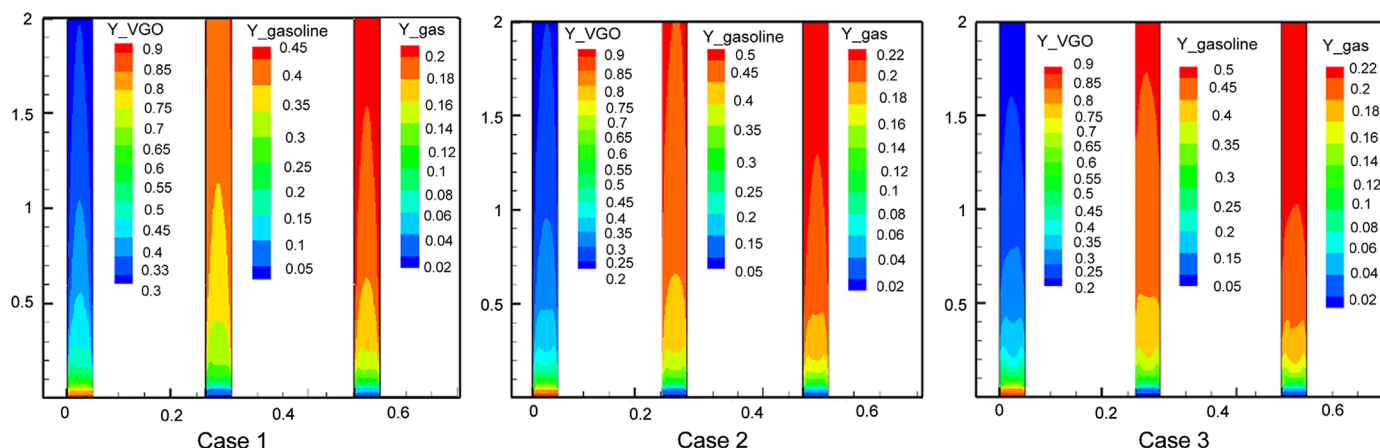


Fig. 15. The species mass fraction contour of the riser.

captured; these behaviors are not described by conventional CFD models. As a result, more realistic flow fields could be obtained. Figs. 11–13 show that the particle volume fraction predicted by the multi-scale model is smaller than that obtained via a pure CFD model in the bottom section of the riser but larger in the middle-upper sections. Corresponding differences in other parameters (i.e., velocity, temperature, and pressure) are also observed.

5.2.2. Two-phase reaction behavior

As described in Section 5.2.1, obvious flow field differences could be found in Cases 1 to 3; these differences could certainly lead to different two-phase reaction behaviors in (Figs. 14–18).

Fig. 14 shows the effectiveness factor distribution of the VGO reaction at specific steady-state time points. The intra-diffusion resistance was found to be significant for the FCC process. Three different reaction zones based on diffusion limitation could be qualitatively identified, namely, the transport-controlled, the reaction-controlled, and the intermediate transition zones; these zones are the same zone divisions in the riser based on the single-particle model (Section 5.1). The zone divisions further demonstrate that the multi-scale approach/model is feasible and

the qualitative trends predicted by the multi-scale approach/model are reliable. The multi-scale model could capture more elaborate reaction behaviors because the intraparticle transfer effects are considered; such effects cannot be obtained by the pure conventional CFD model. From the zone divisions, more detailed interaction relationships between mass, heat, and momentum transfers, as well as chemical reactions, could be observed. For instance, in the transport-controlled zone, intraparticle mass and heat transfer resistance are relatively large. Thus, the VGO reaction rate in this zone was lower than that in the pure CFD model. The space volumes of both the transport-controlled and intermediate transition zones in Case 3 (with intra-diffusion and PSD) were larger than those in Case 2 (with intra-diffusion only) (Fig. 14). The PSD has a significant effect on the reaction behaviors, particularly in the middle-upper section of the FCC riser. In summary, the multi-scale model can predict more realistic and detailed reactions and flow behaviors in FCC risers. The effects of intraparticle transfer with PSD on the yield of products and feed conversion are further analyzed below.

Fig. 15 shows the contours for species mass fractions. Obvious differences may be found in Cases 1 and 2. These differences were significant in the bottom section of the riser ($H < 0.5$ m) and

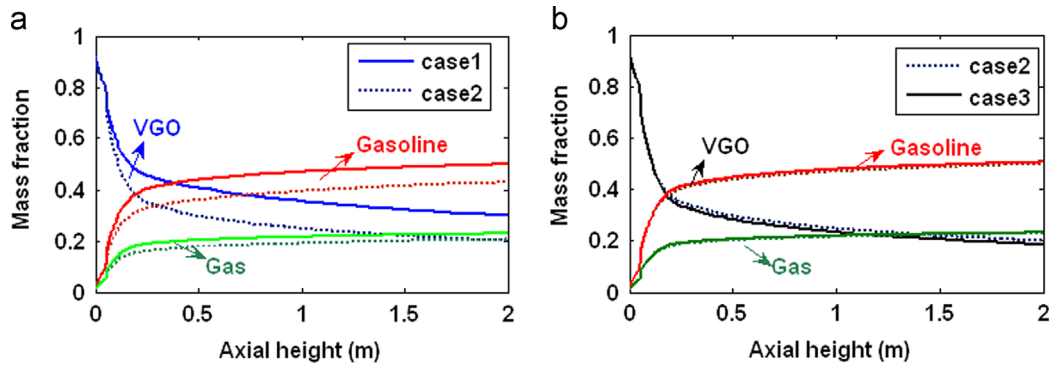


Fig. 16. The species mass fraction axial distribution along the riser height.

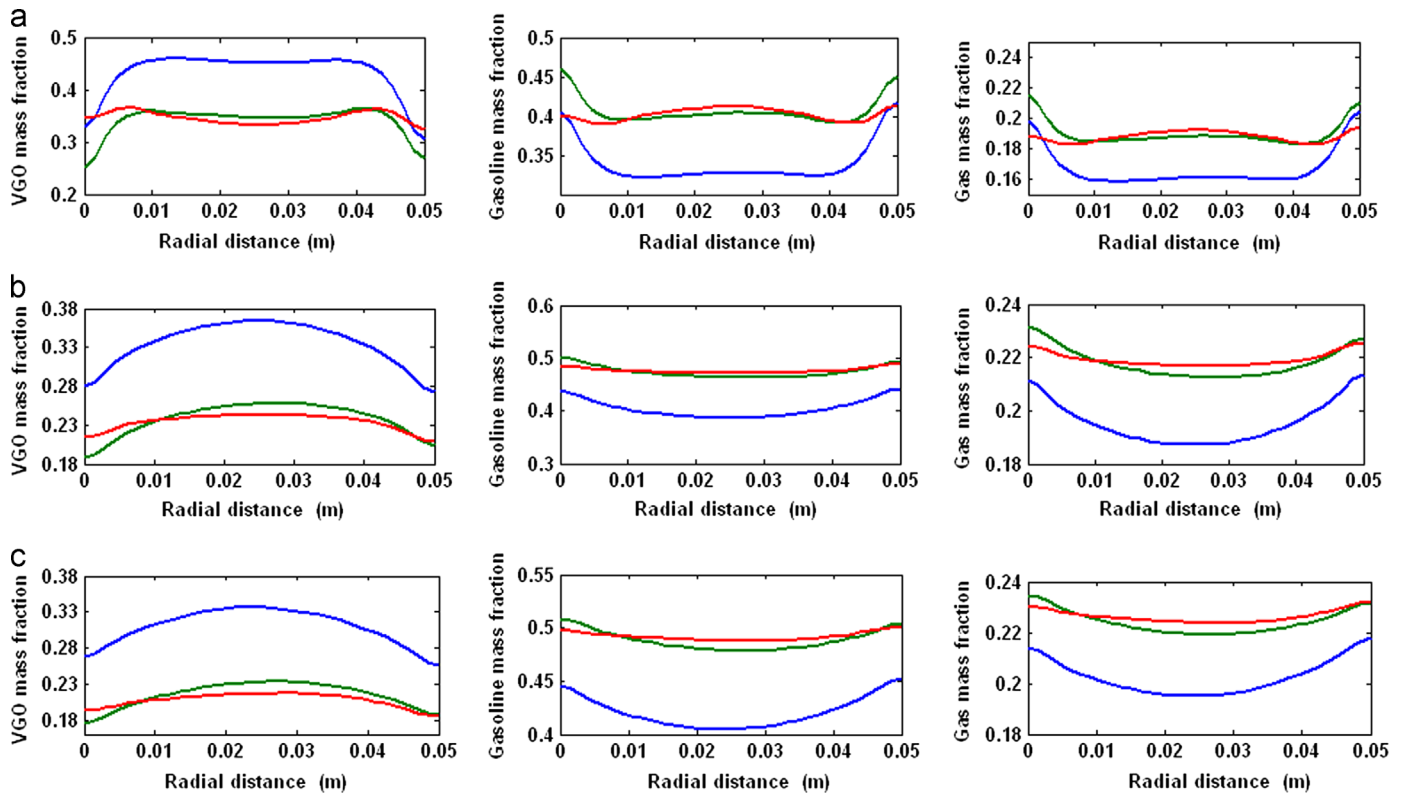


Fig. 17. The species mass fraction radial profiles at different elevations z in the riser ((a) $z=0.25$ m, (b) $z=0.875$ m, (c) $z=1.25$ m).

decreased along the axial direction. This phenomenon corresponds with the decrease in intra-diffusion along the riser height (Figs. 8 and 14). However, the total composition profiles in Cases 2 and 3 were similar at the same axial height. Given that the particle volume fraction in Case 3 was larger than that in Case 2 (Fig. 11(a)), the reaction degree thus increased. The axial and radial composition profiles in Cases 1 to 3 were still different, and these may be observed in Figs. 16 and 17. Fig. 16 shows that all of the axial component concentrations changed rapidly near the riser entrance and gradually in the upper regions. All of the yield non-uniformities in the radial direction could also be observed in Fig. 17 because of solid fraction non-uniformity in the radial direction (Fig. 11(b)–(d)). These results for component concentrations are consistent with those reported in the literature (Gao et al., 1999; Wu et al., 2009; Sharma et al., 2011). Fig. 16 shows that the reaction degree in Case 2 was larger than that in Case 1, and both the gasoline and gas yields in Case 2 were higher than those in Case 1. In practice, given that intraparticle transfer resistance is

considered in Case 2, the reaction rate in this case is lower than that in Case 1, which results in lower mass fractions in Case 2. This phenomenon consequently results in longer catalyst residence times, that is, a deeper reaction degree in Case 2. Fig. 16(a) shows that the effect of intraparticle mass transport resistance was most significant on VGO, followed by gasoline, and then gas. The effect of PSD on all of the components was more significant in the middle-upper section than in any other section of the riser. As described in Fig. 16(b), the effect of PSD on the bottom section of the riser was nearly identical among all cases but deviated slightly in the middle-upper section.

Fig. 17 illustrates simulated radial component differences at typical axial height positions resulting from the application of different sub-models. The simulated VGO fraction in Case 1 was higher than that in Case 2 and higher in Case 3 than in Case 2 near the wall region but lower at the center region. Opposite results were found for the products described in Fig. 17. To investigate the intraparticle transfer effect predicted via the single-particle and

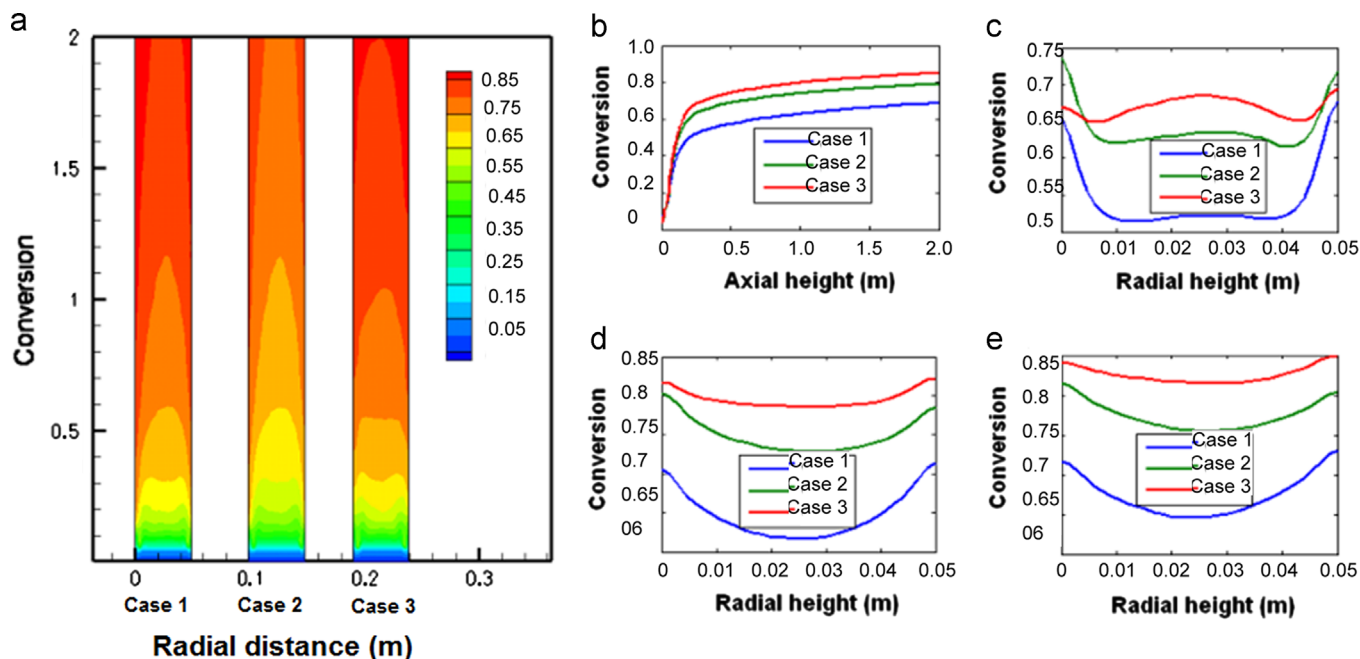


Fig. 18. The feed conversion profiles ((a) the contour plots (b) axial distribution, (c) radial distribution at $z=0.25$ m, (d) radial distribution at $z=0.875$ m, (e) radial distribution at $z=1.25$ m).

PBM sub-models directly, the detailed feed conversion distribution in the riser was predicted using the different models (Fig. 18). Fig. 18(a) shows that the simulated feed conversion in the entire riser was highest in Case 3 and lowest in Case 1. The same results could be found along the riser radial direction except for the distributions near the wall region of the bottom section (Fig. 18(a)–(d)). In summary, the multi-scale model could well capture the qualitative features of the FCC process and produce more elaborate and realistic simulations of reactor behaviors, which are necessary for acquiring new insights.

6. Conclusions

In this study, a multi-scale model comprising a two-phase CFD model, a single-particle model, and PBM was developed to describe turbulent gas–solid flows and reactions in a polydisperse FCC riser reactor. The single-particle and multi-scale models were well verified and evaluated using empirical equations and simple test cases. Comparing the results gives the following conclusions:

- (1) Intraparticle transfer resistance was significant for fast or strongly endothermic reactions (i.e., FCC), and feed conversion was higher than that obtained from simulations using the pure CFD model without the single-particle model. Three different reaction zones, namely, the transport-controlled, reaction-controlled, and intermediate transition zones, were identified based on diffusion limitations in the industrial-scale and laboratory-scale FCC riser reactors. These zones cannot be obtained by the conventional CFD model.
- (2) Particle breakage and aggregation were significant, particularly in the middle-upper sections of the FCC riser. Some particles became smaller and the solid volume became lower than those observed in simulations using the pure CFD model without PBM near the wall regions; other particles formed clusters and the solid volume became larger than that observed in simulations using the pure CFD model without PBM in the central regions. As well, feed conversion was

higher than that obtained from the simulation without PBM, except near the wall regions in the bottom section of the riser.

- (3) Although the multi-scale model and its solution method have been verified and evaluated, the simulation results could not be completely generalized to commercial FCC risers. The proposed model captures the qualitative trends within an FCC riser well and the model is capable of obtaining more elaborate reactor behaviors with relatively low computational cost. This model helps improve the current understanding of the FCC process at a more mechanistic and comprehensive level and provides a viable approach for FCC process intensification and multi-scale reactor modeling studies. The results of this work will be verified in future studies.

In summary, the present work offers new insights into the fundamental macro-scale and meso-scale mechanisms and represents a more systematic and comprehensive study that considers both intraparticle diffusion limitations and catalyst PSD for the FCC process. The multi-scale model could produce more detailed and realistic reactor behaviors and will be helpful in multi-scale reactor modeling.

Nomenclature

A_i	Pre-exponential factor, $\text{m}^6/(\text{mol kg}_{\text{cat}} \text{s})$ for the second order reaction, $\text{m}^3/(\text{kg}_{\text{cat}} \text{s})$ for the first order reaction
C_i	molar concentration of the i th component, mol/m^3
E_i	activation energy of the i th reaction, J/mol
h'	Schiller modulus
ΔH_i	the heat absorbed by the i th reaction, J/kmol
K_i	intrinsic rate constant of the i th reaction, $\text{m}^6/(\text{mol kg}_{\text{cat}} \text{s})$ for the second order reaction and $\text{m}^3/(\text{kg}_{\text{cat}} \text{s})$ for the first order reaction
$Y_{\text{CH}_3\text{OH}}^{\text{int el}}$	molecule weight of the i th component, kg/kmol
\mathfrak{R}_i	rate of the i th reaction, $\text{kmol}/(\text{kg}_{\text{cat}} \text{s})$
T	temperature, K
Y_i	mass fraction of the i th component
Y_i^{s}	the mass fraction of species i in the external of catalyst

η	reaction effectiveness factor
α	catalyst deactivation coefficient
α_{ex}	external surface area of zeolite crystal
ρ	mixed fluid density, kg/m^3
ρ_q	the density of the q th phase, kg/m^3
ρ_{cat}	real catalyst density, kg/m^3
ρ_i	the i th component density, kg/m^3
φ_{t_c}	intrinsic catalyst decay function

Superscript

c the center of the catalyst particle

Acknowledgments

The authors thank the National Ministry of Science and Technology of China (No. 2012CB21500402), the Research Fund for the Doctoral Program of Higher Education (No. 20130073110077), the State Key Laboratory of Coal Conversion of China (No. J13-14-102), and the State-Key Laboratory of Chemical Engineering of Tsinghua University (No. SKL-CHE-13A05) for supporting this work.

Appendix A. Supporting information

Supplementary data associated with this article can be found in the online version at <http://dx.doi.org/10.1016/j.ces.2014.01.015>.

References

- Aris, R., 1969. Elementary chemical reactor analysis, 1st ed. Prentice Hall, Englewood Clis.
- Ali, H., Rohani, S., Corriou, J.P., 1997. Modeling and control of a riser type fluid catalytic cracking (FCC) unit. *Chem. Eng. Technol.* 20, 118–130.
- Al-Khattaf, S., de Lasa, H.I., 1999. Activity and selectivity of fluidized catalytic cracking in a riser simulator: The role of Y-zeolite crystal size. *Ind. Eng. Chem. Res.* 38, 1350–1356.
- Bi, H.T., Li, J.H., 2004. Multiscale analysis and modeling of multiphase chemical reactors. *Adv. Powder Technol.* 15, 607–627.
- Berry, T.A., McKeen, T.R., Pugsley, T.S., Dalai, A.K., 2004. Two-dimensional reaction engineering model of the riser section of a fluid catalytic cracking unit. *Ind. Eng. Chem. Res.* 43, 5571–5581.
- Chen, J.W., Deng, Li, X., Liu, T.J., Sha, Y.X., 2005. Catalytic cracking technology and engineering, 2nd ed. China Petrochemical Press.
- Chen, X.Z., Luo, Z.H., Yan, W.C., Lu, Y.H., Ng, I.S., 2011. Three-dimensional CFD-PBM coupled model of the temperature fields in fluidized bed polymerization reactors. *AIChE J.* 57, 3351–3366.
- Chang, J., Wang, G., Lan, X.Y., Gao, J.S., Zhang, K., 2013. Computational investigation of a turbulent fluidized-bed FCC regenerator. *Ind. Eng. Chem. Res.* 52, 4000–4010.
- Chen, G.Q., Luo, Z.H., Lan, X.Y., Xu, C.M., Gao, J.S., 2013. Evaluating the role of intraparticle mass and heat transfers in a commercial FCC riser: A meso-scale study. *Chem. Eng. J.* 228, 352–365.
- Chen, X.M., Luo, Z.H., Zhu, Y.P., Xiao, J., Chen, X.D., 2013. Direct concurrent multi-scale CFD modeling the effect of intraparticle transfer on the flow field in a MTO FBR. *Chem. Eng. Sci.* 108, 690–700.
- Dollet, A., 2004. Multiscale modeling of CVD film growth—a review of recent works. *Surf. Coat. Tech.* 177–178, 245–251.
- Dompazis, G., Kanellopoulos, V., Touloupides, V., Kiparissides, C., 2008. Development of a multi-scale, multi-phase, multi-zone dynamic model for the prediction of particle segregation in catalytic olefin polymerization FBRs. *Chem. Eng. Sci.* 63, 4735–4753.
- Dutta, A., Constales, D., Heynderickx, G.J., 2012. Applying the direct quadrature method of moments to improve multiphase FCC riser reactor simulation. *Chem. Eng. Sci.* 83, 93–109.
- Gianetto, A., Hany, I., Farag, A.P., Blasetti, H.I., de Lasa, 1994. Fluid catalytic cracking catalyst for reformulated gasolines kinetic modeling. *Ind. Eng. Chem. Res.* 33, 3053–3062.
- Gidaspow, D., 1994. *Multiphase Flow and Fluidization: Continuum and Kinetic Theory Description*. Academic Press, Boston.
- Gao, J.S., Xu, C.M., Lin, S.X., Yang, G.H., 1999. Advanced model for turbulent gas–solid flow and reaction in FCC riser reactors. *AIChE J.* 45, 1095–1113.
- Gupta, A., Rao, D.S., 2003. Effect of feed atomization on FCC performance: simulation of entire unit. *Chem. Eng. Sci.* 58, 4567–4579.
- Gao, J.S., Chang, J., Lu, C.X., Xu, C.M., 2008a. Experimental and computational studies on flow behavior of gas–solid fluidized bed with disparately sized binary particles. *Particuology* 6, 59–71.
- Gao, J.S., Chang, J., Lan, X.Y., Yang, Y., Lu, C.X., Xu, C.M., 2008b. CFD modeling of mass transfer and stripping efficiency in FCCU strippers. *AIChE J.* 54, 1164–1177.
- Gao, J.S., Lan, X.Y., Fan, Y.P., Chang, J., Wang, G., Lu, C.X., Xu, C.M., 2009a. CFD modeling and validation of the turbulent fluidized bed of FCC particles. *AIChE J.* 55, 1680–1694.
- Gao, J.S., Lan, X.Y., Fan, Y.P., Chang, J., Wang, G., Lu, C.X., Xu, C.M., 2009b. Hydrodynamics of gas–solid fluidized bed of disparately sized binary particles. *Chem. Eng. Sci.* 64, 4302–4316.
- Gan, J.Q., Zhao, H., Berrouk, A.S., Yang, C.H., Shan, H.H., 2011. Numerical simulation of hydrodynamics and cracking reactions in the feed mixing zone of a multi-regime gas–solid riser reactor. *Ind. Eng. Chem. Res.* 50, 11511–11520.
- Gilbert, W.R., Morgado, E., Abreu, M.A.S., Puente, G., Passamontib, F., Sedran, U., 2011. A novel fluid catalytic cracking approach for producing low aromatic LCO. *Fuel Process. Technol.* 92, 2235–2240.
- Gao, X., Zhu, Y.P., Luo, Z.H., Guo, A.Y., 2011. CFD modeling of gas flow in porous medium and catalytic coupling reaction from carbon monoxide to diethyl oxalate in fixed-bed reactors. *Chem. Eng. Sci.* 66, 6028–6038.
- Han, I.S., Chung, C.B., 2001. Dynamic modeling and simulation of a fluidized catalytic cracking process. Part II: property estimation and simulation. *Chem. Eng. Sci.* 56, 1973–1990.
- Jacob, S.M., Gross, B., Voitz, S.E., Weekman, V.W., 1976. A lumping and reaction scheme for catalytic cracking. *AIChE J.* 22, 701–713.
- Karger, J., Ruthven, D.M., 1992. *Diffusion in zeolites and other microporous solids*. John Wiley & Sons, New York.
- Kiss, I.Z., Hudson, J.L., 2003. Chemical complexity: spontaneous and engineered structures. *AIChE J.* 49, 2234–2241.
- Lun, C.K.K., Savage, S.B., Jeffrey, D.J., Chepurini, N., 1984. Kinetic theories for granular flow–inelastic particles in couette-flow and slightly inelastic particles in a general flow field. *J. Fluid Mech.* 140, 223–232.
- Lee, L., Chen, Y.T., Huang, W., 1989. Four lump kinetic model for fluid catalytic cracking process. *Can. J. Chem. Eng.* 67, 615–619.
- Li, J.H., Cheng, C.L., Zhang, Z.D., Yuan, J., Nemet, A., Fett, F.N., 1999. The EMMS model—its application, development and updated concepts. *Chem. Eng. Sci.* 54, 5409–5425.
- Li, J.H., Kwauk, M., 2003. Exploring complex systems in chemical engineering—the multi-scale methodology. *Chem. Eng. Sci.* 58, 521–535.
- Lasa, H.D., Salaices, E., Mazumder, J., Lucky, R., 2011. Catalytic steam gasification of biomass: catalysis, thermodynamics and kinetics. *Chem. Rev.* 111, 5404–5433.
- Li, J., Luo, Z.H., Lan, X.Y., Xu, C.M., Gao, J.S., 2013. Numerical simulation of the turbulent gas–solid flow and reaction in a polydisperse FCC riser reactor. *Powder Technol.* 237, 569–580.
- Marroquin, G., Ancheya, J., Esteban, C., 2005. A batch reactor study to determine effectiveness factors of commercial HDS catalyst. *Catal. Today* 104, 70–75.
- Nace, D.M., 1970. Catalytic cracking over crystalline aluminosilicates: Microreactor study of gas oil cracking. *Ind. Eng. Chem. Prod. Res. Dev.* 9, 203–209.
- Nayak, S.V., Joshi, S.L., Ranade, V.V., 2005. Modeling of vaporization and cracking of liquid oil injected in a gas–solid riser. *Chem. Eng. Sci.* 60, 6049–6066.
- Pashikanti, K., Liu, Y.A., 2011. Predictive modeling of large-scale integrated refinery reaction and fractionation systems from plant data. Part 2: Fluid catalytic cracking (FCC) process. *Energy. Fuel* 25, 5298–5319.
- Smith, J.M., 1981. *Chemical engineering kinetics*. McGraw-Hill, New York.
- Sha, Y.X., Chen, X.S., Liu, J.X., Weng, H., Zhu, Z., Mao, X., 1985. Investigation of the lumped kinetic model for catalytic making and the establishment of the physical model. *Acta Petrolei Sin. (Petroleum Process Section)* 1, 3–15.
- Sha, Y.X., Chen, X.S., Liu, J.X., Weng, H., Zhu, Z., Mao, X., 1995. Study on the 13-lump kinetic model for residual catalytic cracking, the selective papers in memorial of 30th anniversary of the fluid catalytic cracking process in China, Luoyan Petrochemical Engineering Corporation, Luoyang, China, p. 145.
- Sadeghbeigi, R., 2000. *Fluid catalytic cracking: Design, operation, and troubleshooting of FCC facilities*. Gulf Publishing Company, Houston.
- Schwarz, M.P., Lee, J., 2007. Reactive CFD simulation of an FCC regenerator. *Asia-Pac. J. Chem. Eng.* 2, 347–354.
- Shi, D.P., Luo, Z.H., Guo, A.Y., 2010. Numerical simulation of the gas–solid flow in fluidized-bed polymerization reactors. *Ind. Eng. Chem. Res.* 9, 4070–4079.
- Solsvik, J., Jakobsen, H.A., 2011. Modeling of multicomponent mass diffusion in porous spherical pellets: application to steam methane reforming and methanol synthesis. *Chem. Eng. Sci.* 66, 1986–2000.
- Sharma, H., Gupta, R.K., Singh, P., 2011. Modeling and simulation of fluid catalytic cracking riser reactor (Master thesis), Thapar University, Patiala, India.
- Takatsuka, T., Sato, S., Morimoto, Y., Hashimoto, H., 1987. A reaction model for fluidized-bed catalytic cracking of residual Oil. *Int. Chem. Eng.* 27, 107–116.
- Venuto, P.B., Habib, E.T., 1979. *Fluid catalytic cracking with zeolite catalysts*. Marcel Dekker, New York.
- Van den Akker, H.E.A., 2010. Toward a truly multiscale computational strategy for simulating turbulent two-phase flow processes. *Ind. Eng. Chem. Res.* 49, 10780–10797.
- Vegndla, S.P., Heynderickx, G.J., Marin, G.B., 2012. Probability density function simulation of turbulent reactive gas–solid flow in a FCC riser. *AIChE J.* 58, 268–284.
- Weekman, V.W., Nace, D.M., 1970. Kinetics of catalytic cracking selectivity in fixed, moving and fluid bed reactors. *AIChE J.* 16, 397–404.
- Wang, L., Yang, B., Wang, Z., 2005. Lumps and kinetics for the secondary reactions in catalytically cracked gasoline. *Chem. Eng. J.* 109, 1–9.

- Wang, W., Li, J.H., 2007. Simulation of gas–solid two-phase flow by a multi-scale CFD approach-Extension of the EMMS model to the sub-grid level. *Chem. Eng. Sci.* 62, 208–231.
- Wu, C.N., Cheng, Y., Jin, Y., 2009. Understanding riser and downer based fluid catalytic cracking processes by a comprehensive two-dimensional reactor model. *Ind. Eng. Chem. Res.* 48, 12–26.
- Wu, C.N., Cheng, Y., Ding, Y.L., Jin, Y., 2010. CFD–DEM simulation of gas–solid reacting flows in fluid catalytic cracking (FCC) process. *Chem. Eng. Sci.* 65, 542–549.
- Wang, G., Chao, Z.T., Lan, X.Y., Wang, W., Xu, C.M., Gao, J.S., 2011. Restricted diffusion of residual molecules in catalyst pores under reactive conditions. *Chem. Eng. Sci.* 66, 1200–1211.
- Xu, C.M., Gao, J.S., Lin, S.X., Yang, G.H., 2002. Analysis of catalytic cracking reaction process. China Petroleum Industry Press, Beijing.
- Yan, W.C., Luo, Z.H., Lu, Y.H., Chen, X.D., 2012a. A CFD–PBM–PMLM integrated model for the gas–solid flow fields in fluidized bed polymerization reactors. *AIChE J.* 58, 1717–1732.
- Yan, W.C., Chen, G.Q., Luo, Z.H., 2012b. A CFD modeling approach to design a new gas-barrier in a multizone circulating polymerization reactor. *Ind. Eng. Chem. Res.* 51, 15132–15144.
- Yan, W.C., Shi, D.P., Luo, Z.H., Lu, Y.H., 2011. Three-dimensional CFD study of liquid–solid flow behaviors in tubular loop polymerization reactors: The effect of guide vane. *Chem.Eng.Sci.* 18, 4127–4137.
- Zhu, K., Mao, X., Weng, H., Zhu Z., Liu, F., 1985. Investigation of the lumped kinetic model for catalytic cracking: II. A prior simulation for experimental planning. *Acta Petrolei Sin. (Petroleum Process Section)* p. 47.
- Zhu, C., Jun, Y., Patel, R., Wang, D.W., Ho, T.C., 2011. Interactions of flow and reaction in fluid catalytic cracking risers. *AIChE J.* 57, 3122–3131.